


Differences in Retinal and Choroidal Microvasculature and Structure in Dementia With Lewy Bodies Compared With Normal Cognition

Suzanna Joseph, BS^{1,2} , Cason B. Robbins, MD^{1,2}, Ariana Allen, BS^{1,2} , Alice Haystead², Angela Hemesath, MSE^{1,2}, Anita Kundu, BS^{1,2}, Justin P. Ma, MD², Kim G. Johnson, MD³, Rupesh Agrawal, MD^{4,5}, Vithiya Gunasan^{4,5}, Sandra S. Stinnett, DrPH^{1,2}, Dilraj S. Grewal, MD, FASRS^{1,2}, and Sharon Fekrat, MD, FASRS^{1,2,3} 

Journal of VitreoRetinal Diseases
2024, Vol. 8(1) 67–74
© The Author(s) 2023
Article reuse guidelines:
sagepub.com/journals-permissions
DOI: 10.1177/24741264231206607
journals.sagepub.com/home/jvrd



Abstract

Purpose: To evaluate the retinal and choroidal microvasculature and structure in individuals with dementia with Lewy bodies (DLB) compared with controls with normal cognition using optical coherence tomography (OCT) and OCT angiography (OCTA). **Methods:** An institutional review board–approved cross-sectional comparison of patients with DLB and cognitively normal controls was performed. The Cirrus HD-OCT 5000 with AngioPlex (Carl Zeiss Meditec) was used to obtain OCT and OCTA images. **Results:** Thirty-four eyes of 18 patients with DLB and 85 eyes of 48 cognitively normal patients were analyzed. The average capillary perfusion density (CPD) was higher in the DLB group than in the control group ($P = .005$). The average capillary flux index (CFI) and ganglion cell inner-plexiform layer (GC-IPL) thickness were lower in the DLB group than in the control group ($P = .016$ and $P = .040$, respectively). **Conclusions:** Patients with DLB had an increased peripapillary CPD, decreased peripapillary CFI, and attenuated GC-IPL thickness compared with those with normal cognition.

Keywords

retina, OCT, OCT angiography, diagnostic test, imaging

Introduction

Dementia with Lewy bodies (DLB) is the second most common cause of neurodegenerative disease after Alzheimer disease, accounting for up to 7.5% of dementia cases.^{1–4} Classically, its cardinal symptoms and signs include recurrent visual hallucinations, fluctuating cognition, rapid eye movement (REM) sleep disorder, and symptoms of parkinsonism such as bradykinesia and rigidity.^{5,6} There is, however, great variability in the relative severity of each of these symptoms.⁷ This makes DLB a challenge to distinguish from other neurocognitive disorders such as Alzheimer disease, Parkinson disease, and mild cognitive impairment.^{7,8}

In an effort to improve diagnostic accuracy, the DLB Consortium, a multinational panel of DLB experts, has created diagnostic guidelines.^{9–11} The best studied of these guidelines is the 2005 Revised Criteria for the Clinical Diagnosis of DLB, which consisted of tiered diagnostic criteria highlighting various clinical symptoms of DLB.¹⁰ Despite its thoughtful construction, this diagnostic tool had a sensitivity of 32.1%.¹² These guidelines were updated in 2017 to include objective diagnostic biomarkers.¹¹ However, only 3 biomarkers (reduced

dopamine transporter uptake in the basal ganglia, abnormal iodine meta-iodobenzylguanidine myocardial scintigraphy, and polysomnography demonstrating REM sleep without atonia) were identified as “indicative.”¹¹ This evident lack of robust objective biomarkers shows the need for more accessible, reliable, and noninvasive biomarkers for DLB.

There has been increasing interest in the identification of retinal biomarkers in neurodegenerative disease.^{13–16} As an extension of the central nervous system, the retina shares a

¹ Department of Ophthalmology, Duke University School of Medicine, Durham, NC, USA

² iMIND Research Group, Durham, NC, USA

³ Department of Neurology, Duke University School of Medicine, Durham, NC, USA

⁴ National Healthcare Group Eye Institute, Tan Tock Seng Hospital, Singapore, Singapore

⁵ Lee Kong Chian School of Medicine, Nanyang Technological University, Singapore, Singapore

Corresponding Author:

Sharon Fekrat, MD, FASRS, Department of Ophthalmology, Duke University School of Medicine, 2351 Erwin Rd, Durham, NC 27710, USA.
Email: iMIND@duke.edu

similar structure to brain tissue with regard to vasculature as well as inflammatory milieu.¹⁷ However, unlike the brain, the retina can be directly visualized, making it an ideal surrogate for monitoring the neuronal changes seen in neurodegenerative disease.¹⁵ There is a growing association between retinal structural alterations and a diagnosis of DLB, with exploratory studies showing phosphorylated alpha-synuclein deposits, parafoveal thinning of the ganglion cell inner-plexiform layer (GC-IPL), and electroretinography alterations.^{18–20}

In this study, we assessed the use of optical coherence tomography (OCT) and OCT angiography (OCTA) to characterize the retinal and choroidal microvasculature and structure in individuals with DLB compared with controls with normal cognition.

Methods

The Duke Health Institutional Review Board approved this study (Pro00082598), which complied with the US Health Insurance Portability and Accountability Act of 1996 and the tenets of the World Medical Association Declaration of Helsinki. Written informed consent was obtained from all participants or a legally authorized representative before study enrollment.

Participants

Prospective study participants were individuals with a clinical diagnosis of DLB. The diagnosis of DLB was established by Duke neurologists specializing in memory disorders after a review of symptomatology, cognitive evaluation, and adjunct testing when available.

Prospective control participants were individuals with no history of neurodegenerative disease or cognitive impairment. Control participants were recruited from the Duke Neurological Disorders Clinic, the Duke Alzheimer's Disease Prevention Registry of research volunteers of normal cognition, and the surrounding community. Participants from the Duke Alzheimer's Disease Prevention Registry were classified as cognitively normal after undergoing an extensive battery of neuropsychological testing.

At the time of imaging, patients and caregivers were queried about a history of ophthalmic and medical conditions, which was then confirmed through medical record review when available. Nonmydriatic ultra-widefield scanning laser ophthalmoscopy imaging (Optos California, Optos) was obtained, and the images were reviewed to exclude participants with retinal pathology. Other exclusion criteria included a history of diabetes mellitus (DM), glaucoma, uncontrolled hypertension, other neurodegenerative disease, a Snellen visual acuity (VA) worse than 20/40 measured at the time of data collection, and a spherical equivalent (SE) of less than -6.00 diopters (D) or greater than $+6.00$ D.

Participants also had a cognitive evaluation with the Mini-Mental State Examination (MMSE) and completed a brief questionnaire, including a family history of neurodegenerative disorders and years of education at the time of image acquisition.

OCTA and OCT Image Acquisition and Protocols

All patients were imaged using the Cirrus HD-OCT 5000 with AngioPlex OCTA (software version 11.0.0.29946, Carl Zeiss Meditec).²¹ The superficial capillary plexus vessel density (VD) and perfusion density (PD) were measured on $3\text{ mm} \times 3\text{ mm}$ and $6\text{ mm} \times 6\text{ mm}$ OCTA scans centered on the fovea. The VD was defined as the total length of perfused vasculature over the area measured, while the PD was defined as a percentage of area of perfused vasculature over the total area measured. Both the VD and PD were measured in an Early Treatment Diabetic Retinopathy Study (ETDRS) grid overlay using either the 3.0 mm ETDRS circle and ring or 6.0 mm ETDRS circle with inner and outer rings. The foveal avascular zone (FAZ) boundaries were automatically detected on the $3\text{ mm} \times 3\text{ mm}$ scan, and the area was recorded. Study staff reviewed all FAZ boundaries and made adjustments when needed. Those that could not be adjusted were excluded from analysis. The radial peripapillary capillary (RPC) plexus, which runs parallel to ganglion cells in the retinal nerve fiber layer (RNFL), was assessed through a series of $4.5\text{ mm} \times 4.5\text{ mm}$ images centered on the optic nerve head.

A thresholding algorithm was applied to the images to create a binary vessel slab. The vessels were linearized into 1-pixel widths, creating a vessel skeleton map. This was then used to calculate the capillary perfusion density (CPD) and capillary flux index (CFI). The CPD was defined as the percentage of perfused capillary vasculature over the area measured. The CFI was defined as a unitless ratio of perfused capillary vasculature weighted by the normalized flow intensity over the area measured. The flow intensity was quantified by vessel pixel brightness in the en face image.²² The CFI represents the proportion of red blood cells in a given area at any point in time.

OCT images were acquired, including a $512\text{ }\mu\text{m} \times 128\text{ }\mu\text{m}$ macular cube, a $200\text{ }\mu\text{m} \times 200\text{ }\mu\text{m}$ optic disc cube, and a 21-line raster scan of the posterior pole (HD-21 line foveal image) with enhanced depth imaging (EDI). The macular cube image was used to calculate the central subfield thickness (CST) and GC-IPL thickness. The CST was defined as the thickness between the retinal pigment epithelium and inner limiting membrane at the fovea. To calculate the average GC-IPL thickness, a 14.13 mm^2 elliptical area was centered on the fovea. The average RNFL thickness was calculated using a 3.46 mm diameter circle centered on the optic disc.

The choroidal vascularity index (CVI) was calculated using the Comprehensive Ocular Imaging Network to analyze high-definition 21-line foveal images with EDI. The CVI was defined as the ratio between the vascular luminal area (LA) and total choroidal area (TCA) and represents the vascularity of the choroid. Methods were previously described by Agrawal et al.²³ The TCA was selected with a polygonal tool, which was then used to segment 1.5 mm of the subfoveal choroidal area. The image was then binarized, converting gray-scale images into binarized images, and the color threshold tool was used to select the dark pixels. The dark pixels selected were defined as the LA. The CVI was then calculated by dividing the LA by the TCA.²⁴

Table 1. Demographics.

Variable	DLB Group (n = 18)	Control Group (n = 48)	P Value
Age (y)			
Mean \pm SD	70.78 \pm 6.75	68.98 \pm 10.92	.977 ^a
Median	71.5	73.0	
Range	58.0, 82.0	32.0, 82.0	
MMSE			
Mean \pm SD	25.78 \pm 3.14	29.46 \pm 1.17	<.001 ^{a,b}
Median	27.0	30.0	
Range	20.0, 29.0	23.0, 30.0	
Male sex, n (%)	10 (55.6)	30 (62.5)	.607 ^c

Abbreviations: DLB, dementia with Lewy bodies; MMSE, Mini-Mental State Examination; n, number of patients.

^aWilcoxon rank sum test.

^bStatistically significant.

^cChi-square test.

All images were manually assessed for quality by trained study staff. Those with poor scan quality (less than 7/10 signal strength index or a significant imaging artifact) based on review were excluded from statistical analysis.

Statistical Analysis

Imaging metrics from patients with DLB were compared with those of controls with normal cognition. Statistical analysis was performed using SAS/STAT software (version 9.4, SAS System for Windows, 2002-2012, SAS Institute Inc). Demographic characteristics were compared to assess for possible confounders. The Fisher exact test of differences between proportions was used for categorical variables, and the Wilcoxon rank sum test was used for continuous variables. Generalized estimating equations (GEEs) were used to compare the imaging parameters between groups, accounting for the correlation between 2 eyes of the same study participant. A *P* value less than 0.05 was considered statistically significant.

Results

In the DLB group, 46 eyes of 23 patients were imaged. Of these, 6 eyes were excluded for the presence of DM, 2 eyes were excluded for the presence of glaucoma, 2 eyes were excluded for a mixed Alzheimer disease and DLB diagnosis, 1 eye was excluded for the presence of a retinal pathology, and 1 eye was excluded for a Snellen VA worse than 20/40. Thus, 34 eyes of 18 patients with DLB and 85 eyes of 48 cognitively normal participants were assessed. Table 1 shows the demographics of the study population. Patients with DLB had lower MMSE scores ($P < .001$). The DLB group and control group were well matched by age ($P = .977$) and sex ($P = .607$).

Table 2 shows the results of the GEE analysis of OCTA parameters. The average CPD was higher in patients with DLB than in controls ($P = .005$). The average CFI was lower in the DLB group than in the control group ($P = .016$). There were no other between-group differences in the OCTA parameters measured.

Table 3 shows the results of the GEE analysis of OCT parameters. The DLB group had a decreased average GC-IPL thickness ($P = .040$) compared with the control group. The 2 groups did not differ in the CST ($P = .705$), average RNFL thickness ($P = .072$), or CVI ($P = .127$). Table 4 shows additional analysis of the quadrant data for the RNFL thickness. The inferior quadrant was significantly thinner in the DLB group than in the control group ($P = .014$).

Conclusions

To our knowledge, this is the first cross-sectional study to use OCTA to evaluate the peripapillary RPC plexus in patients with DLB. We found an increased peripapillary CPD and a decreased peripapillary CFI in patients with DLB compared with those with normal cognition. The repeatability of the peripapillary CPD and CFI has been established in patients with neurodegenerative disease as well as in individuals with normal cognition; therefore, these parameters have the potential to function as noninvasive DLB biomarkers.²⁵ In addition, we found attenuated GC-IPL thickness in patients with DLB, which is consistent with results in previous studies.^{19,26,27}

The increased peripapillary CPD seen in DLB could be partially the result of increased inflammatory and angiogenic signaling, as is seen in other neurodegenerative disorders such as Alzheimer disease and multiple sclerosis.²⁸⁻³¹ This hypothesis is supported by Desai Bradaric et al,³² who reported increased angiogenesis in patients with incidental postmortem tissue findings of Lewy bodies in the absence of parkinsonian or cognitive symptoms (prodromal Lewy body dementia). This shows that increased angiogenesis may be present early in the disease pathogenesis, preceding clinical manifestations.³² Vascular changes could, therefore, be used as a means for early disease detection.³²

Some studies suggest that the increased angiogenesis seen in DLB could be the result of the pathologic activation and dysfunction of microglia, which can mediate angiogenesis in the brain via the secretion of cytokines.³²⁻³⁴ The activation of microglia in DLB could be caused by alpha-synuclein, a major

Table 2. Generalized Estimating Equation Analysis of OCTA Parameters.

OCTA Parameter	DLB Group	Control Group	P Value ^a
3 mm × 3 mm perfusion density			
Eyes (n)	30	85	
Mean ± SD	0.347 ± 0.031	0.355 ± 0.029	.326
Median	0.348	0.356	
Range	0.287, 0.394	0.285, 0.406	
3 mm × 3 mm ring perfusion density			
Eyes (n)	30	85	
Mean ± SD	0.366 ± 0.029	0.375 ± 0.030	.206
Median	0.367	0.378	
Range	0.304, 0.412	0.299, 0.425	
3 mm × 3 mm vessel density (mm⁻¹)			
Eyes (n)	30	85	
Mean ± SD	19.1 ± 1.8	19.7 ± 1.6	.187
Median	19.4	19.7	
Range	15.4, 22.3	15.3, 22.7	
3 mm × 3 mm ring vessel density (mm⁻¹)			
Eyes (n)	30	85	
Mean ± SD	20.1 ± 1.7	20.8 ± 1.7	.103
Median	20.1	20.9	
Range	16.2, 22.7	16.0, 24.2	
6 mm × 6 mm perfusion density			
Eyes (n)	28	85	
Mean ± SD	0.419 ± 0.043	0.423 ± 0.041	.692
Median	0.432	0.434	
Range	0.288, 0.463	0.284, 0.475	
6 mm × 6 mm inner ring perfusion density			
Eyes (n)	28	85	
Mean ± SD	0.406 ± 0.055	0.417 ± 0.045	.372
Median	0.414	0.432	
Range	0.245, 0.458	0.274, 0.478	
6 mm × 6 mm outer ring perfusion density			
Eyes (n)	28	85	
Mean ± SD	0.430 ± 0.040	0.433 ± 0.041	.845
Median	0.441	0.448	
Range	0.310, 0.474	0.294, 0.490	
6 mm × 6 mm vessel density (mm⁻¹)			
Eyes (n)	28	85	
Mean ± SD	17.1 ± 1.7	17.1 ± 2.0	.952
Median	17.5	17.8	
Range	12.1, 19.0	8.4, 19.3	
6 mm × 6 mm inner ring vessel density (mm⁻¹)			
Eyes (n)	28	85	
Mean ± SD	16.9 ± 2.1	17.4 ± 1.7	.272
Median	17.5	17.8	
Range	10.5, 19.1	12.1, 19.5	
6 mm × 6 mm outer ring vessel density (mm⁻¹)			
Eyes (n)	28	85	
Mean ± SD	17.5 ± 1.5	17.6 ± 1.5	.792
Median	17.9	18.1	
Range	12.9, 19.2	12.5, 19.6	
Foveal avascular zone (mm²)			
Eyes (n)	27	85	
Mean ± SD	0.207 ± 0.087	0.220 ± 0.095	.605
Median	0.210	0.200	
Range	0.060, 0.360	0.060, 0.450	

(continued)

Table 2. (continued)

OCTA Parameter	DLB Group	Control Group	P Value ^a
Average capillary perfusion density			
Eyes (n)	28	85	
Mean \pm SD	0.444 \pm 0.015	0.434 \pm 0.015	.005 ^b
Median	0.445	0.437	
Range	0.406, 0.476	0.389, 0.474	
Average capillary flux index			
Eyes (n)	28	85	
Mean \pm SD	0.421 \pm 0.026	0.439 \pm 0.031	.016 ^b
Median	0.424	0.439	
Range	0.365, 0.463	0.363, 0.502	

Abbreviations: DLB, dementia with Lewy bodies; OCTA, optical coherence tomography angiography.

^aP value is based on test of difference between means using generalized estimating equations.

^bStatistically significant.

Table 3. Generalized Estimating Equation Analysis of OCT Parameters.

OCT Parameter	DLB Group	Control Group	P Value ^a
Central subfield thickness (μ m)			
Eyes (n)	32	84	
Mean \pm SD	269.5 \pm 41.0	265.0 \pm 18.6	.705
Median	258.5	267.0	
Range	221.0, 389.0	222.0, 305.0	
Ganglion cell inner plexiform layer average thickness (μ m)			
Eyes (n)	33	83	
Mean \pm SD	74.2 \pm 5.7	77.6 \pm 6.0	.040 ^b
Median	74.0	78.0	
Range	62.0, 97.0	61.0, 91.0	
Retinal nerve fiber layer average thickness (μ m)			
Eyes (n)	32	85	
Mean \pm SD	84.4 \pm 6.9	88.2 \pm 8.7	.072
Median	85.0	88.0	
Range	66.0, 96.0	66.0, 107.0	
Choroidal vascularity index (%)			
Eyes (n)	28	85	
Mean \pm SD	0.664 \pm 0.018	0.658 \pm 0.017	.127
Median	0.662	0.657	
Range	0.623, 0.701	0.618, 0.705	

Abbreviations: DLB, dementia with Lewy bodies; OCT, optical coherence tomography.

^aP value is based on test of difference between means using generalized estimating equations.

^bStatistically significant.

component of Lewy bodies.^{35,36} This pathophysiology of microglia-driven angiogenesis may also extend to the retina given that phosphorylated alpha-synuclein has been observed in the retinas of patients with DLB.^{18,37} We therefore hypothesize that angiogenesis in the peripapillary retina may in part be a response to the deposition of alpha-synuclein in the retina in DLB.

We also found a decreased peripapillary CFI in DLB patients. The CFI represents retinal capillary blood flow.³⁸ Several studies have found decreased cerebral perfusion in patients with DLB.^{39–42} We postulate that this decrease in cerebral perfusion translates to a decrease in retinal perfusion,

which is also seen in Alzheimer disease.⁴³ When coupled with the release of inflammatory cytokines, the decreased retinal perfusion may contribute to a compensatory increase in the peripapillary retinal blood vessel formation seen by the increased CPD. However, the CFI remains reduced, suggesting this compensatory revascularization is insufficient to restore normal blood flow.

Although the RPC plexus serves in part to nourish the RNFL,⁴⁴ there was no change in the average RNFL thickness between individuals with DLB and cognitively normal controls. This finding of peripapillary changes in the setting of normal RNFL thickness has similarly been seen in Parkinson disease, which

Table 4. Generalized Estimating Equation Analysis of RNFL Quadrant Thickness.

RNFL Thickness (μm)	DLB Group	Control Group	P Value ^a
Superior quadrant			
Eyes (n)	31	85	
Mean \pm SD	104.6 \pm 15.36	106.1 \pm 14.15	.817
Median	105.0	105.0	
Min, max	63.0, 133.0	81.0, 143.0	
Temporal quadrant			
Eyes (n)	31	85	
Mean \pm SD	60.52 \pm 10.34	61.07 \pm 9.42	.833
Median	60.0	60.0	
Min, max	40.0, 85.0	42.0, 87.0	
Inferior quadrant			
Eyes (n)	31	85	
Mean \pm SD	104.3 \pm 13.98	113.8 \pm 15.22	.014 ^b
Median	104.0	112.00	
Min, max	74.0, 130.0	80.0, 152.0	
Nasal quadrant			
Eyes (n)	31	85	
Mean \pm SD	68.65 \pm 5.27	72.09 \pm 13.42	.102
Median	69.0	71.0	
Min, max	57.0, 76.0	45.0, 123.0	

Abbreviations: DLB, dementia with Lewy bodies; RNFL, retinal nerve fiber layer.

^aP value is based on test of difference between means using generalized estimating equations.

^bStatistically significant.

may suggest that changes in RPC density may precede changes in RNFL thickness.¹⁴ Previous studies have reported mixed results on the thinning of the RNFL in both DLB and Alzheimer disease.^{45,46} When attenuation of the RNFL was found in Alzheimer disease, it was noted primarily in the superior and inferior quadrants.^{47–49} Similarly, when analyzing the quadrant data of our cohort, we found thinning of the inferior quadrant in the DLB group.

The decreased GC-IPL thickness in our study mirrors findings in previous studies of DLB and prodromal Lewy body dementia.^{19,26,27} The GC-IPL consists of ganglion cell bodies and dendrites in the retina, such as amacrine dendrites.^{50,51} Although the specific mechanism of GC-IPL attenuation has not yet been identified, preclinical animal models of Parkinson disease, which shares a pathogenesis similar to that of DLB, have shown significant loss of amacrine cells.^{2,52} Furthermore, attenuation of the GC-IPL has been reported in Parkinson disease, mild cognitive impairment, and Alzheimer disease.^{53,54} This suggests that GC-IPL attenuation may be secondary to neurodegeneration. Our findings support the claim that GC-IPL attenuation could be a relevant biomarker for DLB.

There are some limitations to this study that should be considered when interpreting the results. Although the neurological diagnoses were made by trained neurologists, there is considerable overlap in clinical presentation among the various forms of dementia. Therefore, all diagnoses have varying levels of uncertainty. A definitive diagnosis of DLB can only be made through postmortem tissue analysis.³ The retinal findings we observed may not be unique to DLB but instead may be representative of nonspecific neurodegeneration. Given our

exclusion criteria, including uncontrolled hypertension, DM, glaucoma, and vitreoretinal pathology, our control patients are not representative of all patients, which at present limits the applicability of these findings to a specific patient subset.

Furthermore, we did not perform visual field testing or intraocular pressure testing to fully assess for glaucoma, which can lead to a reduced peripapillary CPD and CFI. However, patients were screened for glaucoma through patient-reported history, a review of widefield images, and a medical record review. We did not account for image scaling error caused by varying axial lengths (ALs).⁵⁵ However, we excluded individuals with an SE less than -6.00 D or greater than $+6.00$ D. Previous work found that this limits the magnitude of differences seen in OCTA parameters resulting from AL.⁵⁶ In addition, we were unable to image some patients with advanced DLB because they were unable to maintain adequate fixation during imaging, to follow imaging cues provided by study staff, and to maintain proper head positioning.

In conclusion, we found an increased peripapillary CPD, decreased peripapillary CFI, and decreased GC-IPL thickness in patients with DLB compared with those with normal cognition. These findings suggest that retinal imaging metrics have the potential to serve as clinically relevant biomarkers for a diagnosis of DLB.

Ethical Approval

This study is in compliance with the US Health Insurance Portability and Accountability Act of 1996 and the tenets of the World Medical Association Declaration of Helsinki. The Duke Health Institutional Review Board approved this study (Pro00082598).

Statement of Informed Consent

Written informed consent was obtained from all participants or their legally authorized representative.

Declaration of Conflicting Interests

The author(s) declared no potential conflicts of interest with respect to the research, authorship, and/or publication of this article.

Funding

The author(s) disclosed receipt of the following financial support for the research, authorship, and/or publication of this article: This study was supported in part by a Research to Prevent Blindness unrestricted grant.

ORCID iDs

Suzanna Joseph  <https://orcid.org/0000-0002-4495-7221>

Ariana Allen  <https://orcid.org/0000-0001-7320-2381>

Sharon Fekrat  <https://orcid.org/0000-0003-4403-5996>

References

- Baskys A. Lewy body dementia: the litmus test for neuroleptic sensitivity and extrapyramidal symptoms. *J Clin Psychiatry*. 2004; 65(suppl 11):16-22.
- Carrarini C, Russo M, Pagliaccio G, et al. Visual evoked potential abnormalities in dementia with Lewy bodies. *Neurophysiol Clin*. 2021;51(5):425-431. doi:10.1016/j.neucli.2021.02.003
- Zupancic M, Mahajan A, Handa K. Dementia with lewy bodies: diagnosis and management for primary care providers. *Prim Care Companion CNS Disord*. 2011;13(5):26212. doi:10.4088/PCC.11r01190
- Amin J, Holmes C, Dorey RB, et al. Neuroinflammation in dementia with Lewy bodies: a human post-mortem study. *Transl Psychiatry*. 2020;10(1):267. doi:10.1038/s41398-020-00954-8
- Mrak RE, Griffin WS. Dementia with Lewy bodies: definition, diagnosis, and pathogenic relationship to Alzheimer's disease. *Neuropsychiatr Dis Treat*. 2007;3(5):619-625.
- Yousaf T, Dervenoulas G, Valkimadi PE, Politis M. Neuroimaging in Lewy body dementia. *J Neurol*. 2019;266(1):1-26. doi:10.1007/s00415-018-8892-x
- Chin KS, Teodorczuk A, Watson R. Dementia with Lewy bodies: challenges in the diagnosis and management. *Aust NZ J Psychiatry*. 2019;53(4):291-303. doi:10.1177/0004867419835029
- Bousiges O, Blanc F. Biomarkers of dementia with Lewy bodies: differential diagnostic with Alzheimer's disease. *Int J Mol Sci*. 2022;23(12):6371. doi:10.3390/ijms23126371
- McKeith IG, Galasko D, Kosaka K, et al. Consensus guidelines for the clinical and pathologic diagnosis of dementia with Lewy bodies (DLB): report of the consortium on DLB international workshop. *Neurology*. 1996;47(5):1113-1124. doi:10.1212/wnl.47.5.1113
- McKeith IG, Dickson DW, Lowe J, et al. Diagnosis and management of dementia with Lewy bodies: third report of the DLB Consortium. *Neurology*. 2005;65(12):1863-1872. doi:10.1212/01.wnl.0000187889.17253.b1
- McKeith IG, Boeve BF, Dickson DW, et al. Diagnosis and management of dementia with Lewy bodies: Fourth consensus report of the DLB Consortium. *Neurology*. 2017;89(1):88-100. doi:10.1212/wnl.0000000000004058
- Nelson PT, Jicha GA, Kryscio RJ, et al. Low sensitivity in clinical diagnoses of dementia with Lewy bodies. *J Neurol*. 2010;257(3): 359-366. doi:10.1007/s00415-009-5324-y
- Yoon SP, Grewal DS, Thompson AC, et al. Retinal microvascular and neurodegenerative changes in Alzheimer's disease and mild cognitive impairment compared with control participants. *Ophthalmol Retina*. 2019;3(6):489-499. doi:10.1016/j.oret.2019.02.002
- Robbins CB, Grewal DS, Thompson AC, et al. Identifying peripapillary radial capillary plexus alterations in Parkinson's disease using OCT angiography. *Ophthalmol Retina*. 2022;6(1):29-36. doi:10.1016/j.oret.2021.03.006
- Snyder PJ, Alber J, Alt C, et al. Retinal imaging in Alzheimer's and neurodegenerative diseases. *Alzheimers Dement*. 2021;17(1): 103-111. doi:10.1002/alz.12179
- Jiang H, Delgado S, Liu C, et al. In vivo characterization of retinal microvascular network in multiple sclerosis. *Ophthalmology*. 2016;123(2):437-438. doi:10.1016/j.ophtha.2015.07.026
- London A, Benhar I, Schwartz M. The retina as a window to the brain—from eye research to CNS disorders. *Nat Rev Neurol*. 2013;9(1):44-53. doi:10.1038/nrneurol.2012.227
- Beach TG, Carew J, Serrano G, et al. Phosphorylated alpha-synuclein-immunoreactive retinal neuronal elements in Parkinson's disease subjects. *Neurosci Lett*. 2014;571:34-38. doi:10.1016/j.neulet.2014.04.027
- Murueta-Goyena A, Del Pino R, Reyero P, et al. Parafoveal thinning of inner retina is associated with visual dysfunction in Lewy body diseases. *Mov Disord*. 2019;34(9):1315-1324. doi:10.1002/mds.27728
- Maurage CA, Ruchoux MM, de Vos R, Surguchov A, Destee A. Retinal involvement in dementia with Lewy bodies: a clue to hallucinations? *Ann Neurol*. 2003;54(4):542-547. doi:10.1002/ana.10730
- Rosenfeld PJ, Durbin MK, Roisman L, et al. ZEISS Angioplex™ spectral domain optical coherence tomography angiography: technical aspects. *Dev Ophthalmol*. 2016;56:18-29. doi:10.1159/000442773
- Chang R, Chu Z, Burkemper B, et al. Effect of scan size on glaucoma diagnostic performance using OCT angiography en face images of the radial peripapillary capillaries. *J Glaucoma*. 2019; 28(5):465-472. doi:10.1097/ijg.0000000000001216
- Agrawal R, Gupta P, Tan KA, Cheung CM, Wong TY, Cheng CY. Choroidal vascularity index as a measure of vascular status of the choroid: measurements in healthy eyes from a population-based study. *Sci Rep*. 2016;6:21090. doi:10.1038/srep21090
- Betzler BK, Ding J, Wei X, et al. Choroidal vascularity index: a step towards software as a medical device. *Br J Ophthalmol*. 2022;106(2):149-155. doi:10.1136/bjophthalmol-2021-318782
- Ma JP, Robbins CB, Stinnett SS, et al. Repeatability of peripapillary OCT angiography in neurodegenerative disease. *Ophthalmol Sci*. 2021;1(4):100075. doi:10.1016/j.xops.2021.100075
- Lee JY, Ahn J, Oh S, et al. Retina thickness as a marker of neurodegeneration in prodromal lewy body disease. *Mov Disord*. 2020;35(2):349-354. doi:10.1002/mds.27914

27. Fragiaco F, Miant S, Pengo M, et al. Clinical and cognitive correlates of selective regional retinal thinning in dementia with lewy bodies. *Mov Disord.* 2019;34(10):1582-1583. doi:10.1002/mds.27851
28. Desai BS, Schneider JA, Li JL, Carvey PM, Hendey B. Evidence of angiogenic vessels in Alzheimer's disease. *J Neural Transm (Vienna).* 2009;116(5):587-597. doi:10.1007/s00702-009-0226-9
29. Thirumangalakudi L, Samany PG, Owoso A, Wiskar B, Grammas P. Angiogenic proteins are expressed by brain blood vessels in Alzheimer's disease. *J Alzheimers Dis.* 2006;10(1):111-118. doi:10.3233/jad-2006-10114
30. Holley JE, Newcombe J, Whatmore JL, Gutowski NJ. Increased blood vessel density and endothelial cell proliferation in multiple sclerosis cerebral white matter. *Neurosci Lett.* 2010;470(1):65-70. doi:10.1016/j.neulet.2009.12.059
31. Taylor JP, McKeith IG, Burn DJ, et al. New evidence on the management of Lewy body dementia. *Lancet Neurol.* 2020;19(2):157-169. doi:10.1016/S1474-4422(19)30153-X
32. Desai Bradaric B, Patel A, Schneider JA, Carvey PM, Hendey B. Evidence for angiogenesis in Parkinson's disease, incidental Lewy body disease, and progressive supranuclear palsy. *J Neural Transm (Vienna).* 2012;119(1):59-71. doi:10.1007/s00702-011-0684-8
33. Mackenzie IR. Activated microglia in dementia with Lewy bodies. *Neurology.* 2000;55(1):132-134. doi:10.1212/wnl.55.1.132
34. Streit WJ, Xue QS. Microglia in dementia with Lewy bodies. *Brain Behav Immun.* 2016;55:191-201. doi:10.1016/j.bbi.2015.10.012
35. Zhang W, Wang T, Pei Z, et al. Aggregated alpha-synuclein activates microglia: a process leading to disease progression in Parkinson's disease. *FASEB J.* 2005;19(6):533-542. doi:10.1096/fj.04-2751com
36. Fellner L, Irschick R, Schanda K, et al. Toll-like receptor 4 is required for α -synuclein dependent activation of microglia and astroglia. *Glia.* 2013;61(3):349-360. doi:10.1002/glia.22437
37. Spillantini MG, Schmidt ML, Lee VM, Trojanowski JQ, Jakes R, Goedert M. Alpha-synuclein in Lewy bodies. *Nature.* 1997;388(6645):839-840. doi:10.1038/42166
38. Abdolahi F, Zhou X, Ashimatey BS, et al. Optical coherence tomography angiography-derived flux as a measure of physiological changes in retinal capillary blood flow. *Transl Vis Sci Technol.* 2021;10(9):5. doi:10.1167/tvst.10.9.5
39. Imamura T, Ishii K, Sasaki M, et al. Regional cerebral glucose metabolism in dementia with Lewy bodies and Alzheimer's disease: a comparative study using positron emission tomography. *Neurosci Lett.* 1997;235(1-2):49-52. doi:10.1016/s0304-3940(97)00713-1
40. Albin RL, Minoshima S, D'Amato CJ, Frey KA, Kuhl DA, Sima AA. Fluoro-deoxyglucose positron emission tomography in diffuse Lewy body disease. *Neurology.* 1996;47(2):462-466. doi:10.1212/wnl.47.2.462
41. Pasquier J, Michel BF, Brenot-Rossi I, Hassan-Sebbag N, Sauvan R, Gastaut JL. Value of (99m)Tc-ECD SPET for the diagnosis of dementia with Lewy bodies. *Eur J Nucl Med Mol Imaging.* 2002;29(10):1342-1348. doi:10.1007/s00259-002-0919-x
42. Yoshida T, Mori T, Yamazaki K, et al. Relationship between regional cerebral blood flow and neuropsychiatric symptoms in dementia with Lewy bodies. *Int J Geriatr Psychiatry.* 2015;30(10):1068-1075. doi:10.1002/gps.4263
43. Lahme L, Esser EL, Mihailovic N, et al. Evaluation of ocular perfusion in Alzheimer's disease using optical coherence tomography angiography. *J Alzheimers Dis.* 2018;66(4):1745-1752. doi:10.3233/jad-180738
44. Yu PK, Cringle SJ, Yu DY. Correlation between the radial peripapillary capillaries and the retinal nerve fibre layer in the normal human retina. *Exp Eye Res.* 2014;129:83-92. doi:10.1016/j.exer.2014.10.020
45. Moreno-Ramos T, Benito-León J, Villarejo A, Bermejo-Pareja F. Retinal nerve fiber layer thinning in dementia associated with Parkinson's disease, dementia with Lewy bodies, and Alzheimer's disease. *J Alzheimers Dis.* 2013;34(3):659-664. doi:10.3233/jad-121975
46. Pillai JA, Bermel R, Bonner-Jackson A, et al. Retinal nerve fiber layer thinning in Alzheimer's disease: a case-control study in comparison to normal aging, Parkinson's disease, and non-Alzheimer's dementia. *Am J Alzheimers Dis Other Dement.* 2016;31(5):430-436. doi:10.1177/1533317515628053
47. Lian TH, Jin Z, Qu YZ, et al. The relationship between retinal nerve fiber layer thickness and clinical symptoms of Alzheimer's disease. *Front Aging Neurosci.* 2020;12:584244. doi:10.3389/fnagi.2020.584244
48. Liu D, Zhang L, Li Z, et al. Thinner changes of the retinal nerve fiber layer in patients with mild cognitive impairment and Alzheimer's disease. *BMC Neurol.* 2015;15:14. doi:10.1186/s12883-015-0268-6
49. Bambo MP, Garcia-Martin E, Pinilla J, et al. Detection of retinal nerve fiber layer degeneration in patients with Alzheimer's disease using optical coherence tomography: searching new biomarkers. *Acta Ophthalmol.* 2014;92(7):e581-e582. doi:10.1111/aos.12374
50. López-de-Eguileta A, Lage C, López-García S, et al. Ganglion cell layer thinning in prodromal Alzheimer's disease defined by amyloid PET. *Alzheimers Dement (N Y).* 2019;5:570-578. doi:10.1016/j.trci.2019.08.008
51. Kolb H. Inner plexiform layer. In: Kolb H, Fernandez E, Nelson R, eds. *Webvision: The Organization of the Retina and Visual System* [Internet]. University of Utah Health Sciences Center; 2001. <https://www.ncbi.nlm.nih.gov/books/NBK11536/>
52. Cuenca N, Herrero MT, Angulo A, et al. Morphological impairments in retinal neurons of the scotopic visual pathway in a monkey model of Parkinson's disease. *J Comp Neurol.* 2005;493(2):261-273. doi:10.1002/cne.20761
53. López-de-Eguileta A, Cerveró A, Ruiz de Sabando A, Sánchez-Juan P, Casado A. Ganglion cell layer thinning in Alzheimer's disease. *Medicina (Kaunas).* 2020;56(10):553. doi:10.3390/medicina56100553
54. Živković M, Dayanir V, Stamenović J, et al. Retinal ganglion cell/inner plexiform layer thickness in patients with Parkinson's disease. *Folia Neuropathol.* 2017;55(2):168-173. doi:10.5114/fn.2017.68584
55. Llanas S, Linderman RE, Chen FK, Carroll J. Assessing the use of incorrectly scaled optical coherence tomography angiography images in peer-reviewed studies: a systematic review. *JAMA Ophthalmol.* 2020;138(1):86-94. doi:10.1001/jamaophthalmol.2019.4821
56. Sampson DM, Gong P, An D, et al. Axial length variation impacts on superficial retinal vessel density and foveal avascular zone area measurements using optical coherence tomography angiography. *Invest Ophthalmol Vis Sci.* 2017;58(7):3065-3072. doi:10.1167/iovs.17-21551